Exploration Geophysics

ISSN: 0812-3985 (Print) 1834-7533 (Online) Journal homepage: https://www.tandfonline.com/loi/texg20

Surface wave analysis: improving the accuracy of the shear-wave velocity profile through the efficient joint acquisition and Full Velocity Spectrum (FVS) analysis of Rayleigh and Love waves

Giancarlo Dal Moro

To cite this article: Giancarlo Dal Moro (2019) Surface wave analysis: improving the accuracy of the shear-wave velocity profile through the efficient joint acquisition and Full Velocity Spectrum (FVS) analysis of Rayleigh and Love waves, Exploration Geophysics, 50:4, 408-419, DOI: 10.1080/08123985.2019.1606202

To link to this article: https://doi.org/10.1080/08123985.2019.1606202

Published online: 04 Jun 2019.

EXPLORATION GEOPHYSICS
2019, VOL. 50, NO. 4, 408–419
https://doi.org/10.1080/08123985.2019.1606202

Taylor & Francis
Taylor & Francis Group

Surface wave analysis: improving the accuracy of the shear-wave velocity profile through the efficient joint acquisition and Full Velocity Spectrum (FVS) analysis of Rayleigh and Love waves

Giancarlo Dal Moro

Department of Seismotectonics, Institute of Rock Structure and Mechanics, Academy of Sciences of the Czech Republic, Prague 8, Czech Republic

ABSTRACT

Surface wave propagation can be exploited to investigate subsurface conditions in terms of shear wave velocities in a number of possible applications (geotechnical site characterisation, seismic-risk assessment, crustal studies and non-destructive testing). Nowadays, one of the most common methods adopted to analyse the dispersion of surface waves is based on the determination of the Rayleigh wave frequency-dependent phase velocities obtained from multichannel active data. The obtained values represent the dispersion curve, which is inverted to determine the vertical shear-wave velocity (V_S) profile. After briefly recalling some fundamental facts and problems regarding surface wave propagation and analysis, we present the Full Velocity Spectrum (FVS) approach which here is used to jointly invert the velocity spectra of the Rayleigh and Love waves acquired by means of a set of horizontal geophones only (Rayleigh waves are in fact analysed while considering their radial component). It is shown that for non-trivial data sets for which modal dispersion curves cannot be soundly extracted, the joint FVS approach may represent an efficient way to properly analyse the data, thus eventually obtaining a robust V_S profile free from significant ambiguities that would otherwise inevitably affect the results obtained by following the ordinary approach based on the modal dispersion curve(s) of just one component.

ARTICLE HISTORY
Received 8 September 2017
Accepted 16 August 2018

KEYWORDS
Surface waves; Rayleigh waves; Love waves; full velocity spectrum (FVS) analysis; joint analysis; multi-component analysis

Introduction

Nowadays, analysis of surface wave dispersion is adopted to derive the vertical shear-wave velocity (V_S) profile in a number of geotechnical and geophysical applications. The method is fundamentally based on the fact that, in a layered medium, short wavelengths (high frequencies) are influenced by shallow layers, whereas longer wavelengths (low frequencies) sense deeper strata. Considering a vertical impact force, more than two-thirds of the produced seismic energy propagates as surface waves (Miller and Pursey 1955), which consequently dominate the wavefield, also suffering from lower attenuation with respect to body waves. The Multichannel Analysis of Surface Wave (MASW) approach (e.g. Park, Miller, and Xia 1999) was originally developed by considering an active vertical source and vertical geophones commonly used also for P-wave reflection and refraction studies. Such a classical approach is therefore based on the analysis of the vertical component of Rayleigh waves only, so that the acronym MASW has somehow become a synonym of "analysis of the modal dispersion curve(s) of the vertical component of Rayleigh waves". During past decades, many other possible methodologies have been implemented based on both active and passive data. Active seismics (Ganji, Gucunski, and Nazarian 1998; Park, Miller, and Xia 1998, Park et al. 2000; Shtivelman 2002; Stokoe et al. 1988), clearly requires a source (sledgehammer, weight drop, explosive charge or vibrating source) and is typically used for the analysis of high frequencies, which for geotechnical applications are usually between 4 and 50 Hz (Dou and Ajo-Franklin 2014; Forbriger 2003a, 2003b) while in case of non-destructive testing for pavement evaluation can reach several hundred Hz (e.g. Ryden and Park 2006). Acquisition parameters (number of geophones and spacing, minimum offset, recording time and sampling rate) depend on the scope of the survey (the larger the array length, the greater the investigated depth).

Passive techniques exploit the background ambient wavefield generated by microtremors and/or cultural activities using a linear array (Louie 2001) or a two-dimensional (2D) deployment of sensors (Aki 1957; Asten 2006; Asten et al. 2014; Capon 1969; Cho, Senna, and Fujiwara 2013; Ling and Okada 1993; Ohori, Nobata, and Wakamatsu 2002; Poggi and Fäh 2010). These methods are aimed mainly at retrieving the dispersive properties of the low frequencies, and their performances depend on the dimensions of the array, the recording time, the characteristics of the microtremor

CONTACT Giancarlo Dal Moro dalmoro@irsm.cas.cz, gdm@winmasw.com Department of Seismotectonics, Institute of Rock Structure and Mechanics, Academy of Sciences of the Czech Republic, V Holešovičkách 94/41, 18209, Prague 8, Czech Republic

field and the quality of both the sensors and the acquisition system. Because linear arrays cannot handle the unknown location of passive seismic sources, analyses based on bi-dimensional arrays necessarily provide clearer velocity spectra (Dal Moro 2014; Ohori, Nobata, and Wakamatsu 2002; Poggi and Fäh 2010).

In the classical approach, processing is fundamentally accomplished through three main steps:

(1) computation of the phase–velocity spectrum from the field data;
(2) interpretation of the phase–velocity spectrum in terms of modal dispersion curve(s);
(3) inversion of the interpreted dispersion curve(s).

During the first step, field records are transformed from the time-offset domain (e.g. Figure 1b) into the velocity–frequency domain (Figure 1c). In the second step, the obtained velocity spectrum is interpreted in terms of dispersion curves, which are picked so to obtain a series of frequency–velocity points depicting the interpreted dispersion curves(s). This is clearly a critical step since an erroneous interpretation would necessarily lead to meaningless results (Zhang and Chan 2003).

As a third and final step, the vertical shear-wave velocity profile is determined by means of an inversion procedure that eventually provides a subsurface model whose theoretical dispersion curves match those picked.

Despite the cost-effectiveness of surface-wave acquisition, intrinsic issues like non-uniqueness of the solution and erroneous velocity spectra interpretation can seriously undermine the overall accuracy of the obtained subsurface model (Dal Moro 2011, 2014; Dal Moro and Ferigo 2011; Zhang and Chan 2003).

About the problems of the velocity spectra interpretation (dispersion curve picking), it must be underlined that the continuity of a signal does not necessarily mean that such a signal pertains to a single mode. In fact, especially when dealing with Rayleigh waves, mode excitation can be extremely complex and, as a consequence, the velocity spectra can be impossible to interpret in terms of modal dispersion curves (see also Chapter 3 in Dal Moro 2014; Dal Moro, Moura, and Moustafa 2015a).

In Figure 1 the data of a synthetic model are presented with the aim of illustrating how complex and counterintuitive interpretation of a classical phase–velocity spectrum, as defined according to the classical MASW approach, can be. The model reported in Figure 1(a) is used to generate the seismic traces reported in Figure 1(b). The velocity spectrum obtained via phase shift (Dal Moro et al. 2003; Park, Miller, and Xia 1998) and reported in Figure 1(c) is apparently clear and continuous (no jump or discontinuity is evident). Despite this, once we plot the theoretical modal dispersion curves of the first two modes, we realise that the signal that dominates the velocity spectrum (Figure 1c) is actually composed of the fundamental mode for a frequency higher than 40 Hz and of the first higher mode for lower frequencies.

Some authors (e.g. Gao et al. 2016; Xia et al. 2006) have named such a phenomenon mode kissing, and a series of further examples is presented in Dal Moro (2014). Given the continuity of the signal along the velocity spectrum (Figure 1c), it is clear that if this data set were to be processed in terms of modal dispersion curves, it would be inevitably misinterpreted, eventually leading to an erroneous subsurface model. In other words, the interpretation and analysis of data sets according to the modal dispersion curves (in these cases, the different modes cannot be separated) and while considering one single component (usually the vertical component of Rayleigh waves), risk being misleading and consequently provide erroneous subsurface models.

A possible solution to these problems is represented by the acquisition and joint analysis of multicomponent data that can be analysed not necessarily by considering interpreted (picked) dispersion curves.

Joint analysis is then important both to better understand each single velocity spectrum (i.e. the way modes interact and possible unify), and to reduce the non-uniqueness of the solution, which necessarily affects the solution even if modal dispersion curves are interpreted properly (Dal Moro 2011, 2014; Ivanov et al. 2006).

In this paper, we consider both Rayleigh and Love waves (Dal Moro and Ferigo 2011; Dal Moro, Moura, and Moustafa 2015a; Safani et al. 2005; Winsborrow, Huwsa, and Muyzert 2003; Xia et al. 2012), and the data are not analysed considering the traditional interpretation–picking–inversion approach but through the Full Velocity Spectrum (FVS) analysis (Dal Moro 2014; Dal Moro et al. 2016; Dal Moro, Coviello, and Del Carlo 2014).

As a matter of fact,, surface waves can be recorded by using different combinations of sources and receivers. For acquisition of the Rayleigh and Love waves analysed here, we used a set of horizontal geophones that allow the recording of both the radial component of Rayleigh waves and Love waves (vertical geophones can be used to record only the vertical component of Rayleigh waves).

We considered the two simple settings depicted in Figure 2:

Rayleigh waves: the axis of the horizontal geophones is oriented parallel to the array and a vertical-impact source is used;

Love waves: horizontal geophones are rotated with the axis perpendicular to the array and Love waves are produced by means of a horizontal (shear) source (a classical wooden beam).

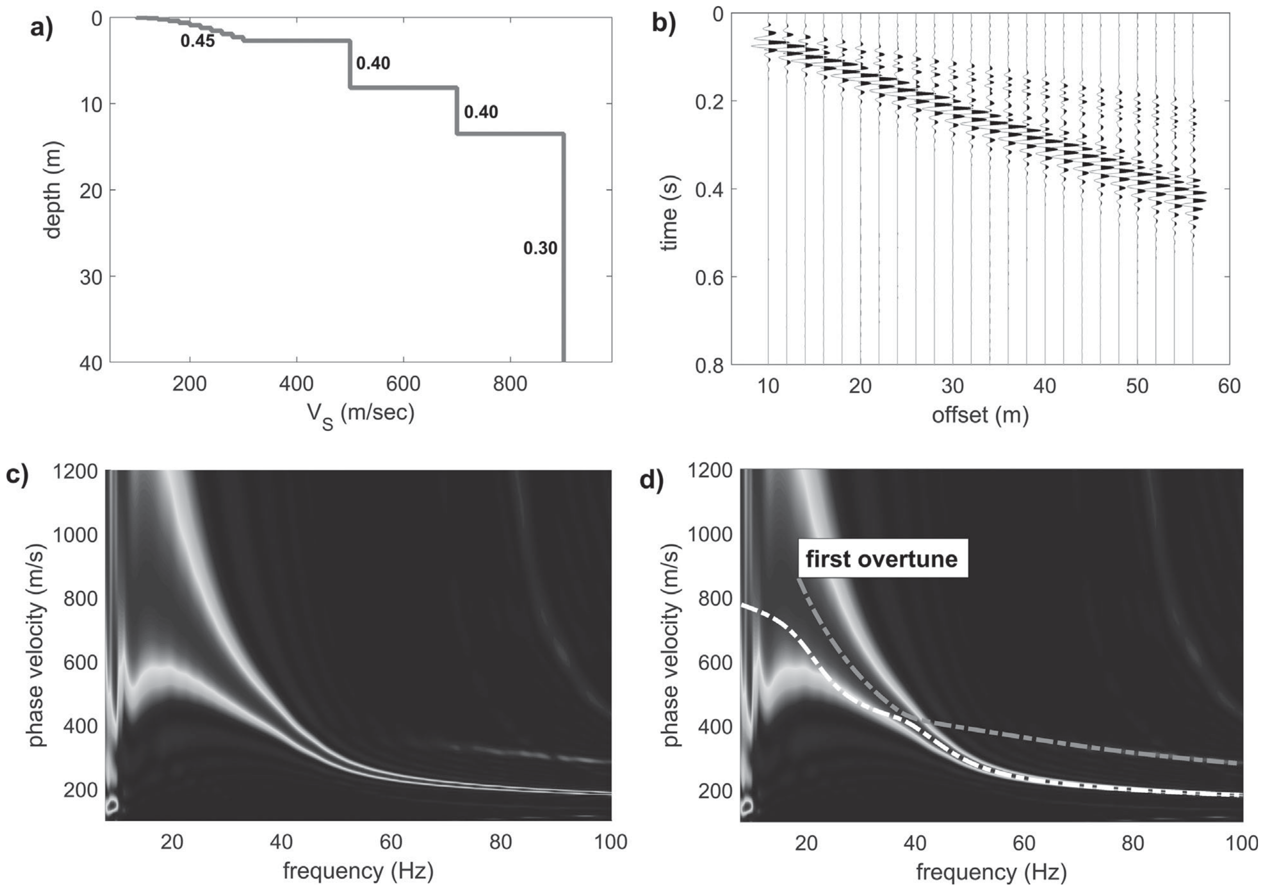

Figure 1. Counterintuitive (and thus misleading) phase–velocity spectrum for a synthetic data set (MASW data): (a) subsurface model (numbers report the adopted Poisson's ratios); (b) synthetic seismic traces computed according to Carcione (1992) (vertical component); (c) phase–velocity spectrum of the synthetic traces computed according to the phase shift method (Park, Miller, and Xia 1998; the values of the obtained matrix represent the normalised summed amplitude for each frequency/velocity point); (d) phase–velocity spectrum and theoretical modal dispersion curves for the first two modes. Because the signal in the velocity spectrum is continuous (see plot c), it is clearly not possible to separate the two modes that dominate the velocity spectrum (fundamental mode for frequencies higher than 40 Hz and first higher mode for lower frequencies – see text for details).

Such a procedure allows a fast and efficient acquisition of Rayleigh (radial component) and Love waves using just a single set of 4.5 Hz horizontal geophones set up according to the scheme reported in Figure 2 and with no need for a set of vertical geophones (which would require more complex field procedures).

Following the coding system originally proposed by Herrmann (2015) and widely adopted in Dal Moro (2014) and Dal Moro, Moura, and Moustafa (2015a, 2016), these two components are abbreviated to RVF and THF: the first letter indicates the type and orientation of the geophones, whereas the second and third letters relate to the source (see Table 1 and Figure 2).

It is important to point out that the velocity spectra of the radial (R) and vertical (Z) components of Rayleigh waves are generally different and it is not possible to state that one component is "better" than the other. If we wish to think in terms of modal dispersion curves, the velocity spectrum of the radial component is sometimes easier to understand than the vertical component, and sometimes the opposite is true (for a wider overview about these issues see Dal Moro 2014; Dal Moro, Moura, and Moustafa 2015a).

After briefly describing the adopted FVS joint approach, we present, comment and invert a field data set with the overall goal of highlighting the two main points that characterize the proposed approach:

(1) joint FVS inversion of Rayleigh and Love waves can be used to handle complex data sets that cannot be solved through the standard method based on interpreted modal dispersion curves of a single component;
(2) the field procedures for efficiently recording the two considered components are extremely straightforward and require the use of just a set of horizontal geophones (it will be shown that for common geotechnical applications a dozen of traces are sufficient).

Inversion method: the FVS approach in a bi-objective perspective

As briefly reported in the introductory paragraph, the analysis of surface wave dispersion via modal dispersion analysis can be quite problematic because the way

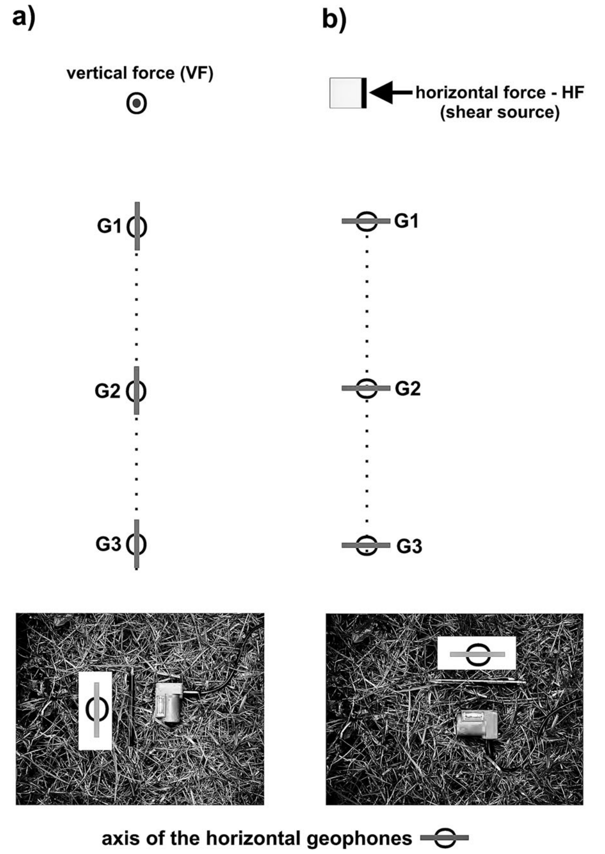

Figure 2. Acquisition of Rayleigh and Love waves using only horizontal component geophones (map view): (a) acquisition of the radial component of Rayleigh waves (the axis of the geophones is set parallel to the array and a vertical force, e.g. a sledgehammer or weight drop, is applied); (b) the geophones are rotated by 90° and a horizontal force is applied.

energy is actually distributed among different modes can be extremely complex and counterintuitive. For this reason, in Dal Moro, Coviello, and Del Carlo (2014) and Dal Moro (2014) a different approach is introduced, based on the analysis of the whole velocity spectrum without the interpretation of the velocity spectra in terms of modal dispersion curves. Such methodology is based on the analysis (inversion) of the whole velocity spectrum (or spectra, in case of multicomponent data) and for this reason, is referred to as Full Velocity Spectrum (FVS) analysis.

Such a method is actually similar to the full-wavefield inversion described in Dou and Ajo-Franklin (2014) for the analysis of seismic data collected in a permafrost region, so that it is somehow possible to speak of a multiple independent creation. Here, synthetics are computed via modal summation and two components (Love waves and the radial component of Rayleigh waves) are analysed jointly.

The FVS approach fundamentally consists of three steps:

(1) computation of the synthetic traces of the considered component(s) (for instance the radial component of Rayleigh waves and/or Love waves) for a tentative model;
(2) determination of the velocity spectra of the computed synthetic traces;
(3) computation of the misfit between the velocity spectra of the field and synthetic traces.

These three steps are implemented within a heuristic optimisation scheme (Coello Coello 2003; Van Veldhuizen and Lamont 2000) that minimises the misfit, thus eventually providing the subsurface model that has a velocity spectrum as close as possible to the velocity spectrum of the field data. It is clearly important to understand that in this way we deal with the entire velocity spectrum (i.e. the frequency–velocity matrix) and not with a dispersion curve (i.e. a frequency–velocity curve that represents a mere subjective interpretation of the velocity spectrum). Figure 3 reports an example of single-component FVS analysis and intends to briefly (and visually) express how, during the FVS inversion process, we aim at identifying a subsurface model whose velocity spectrum is as close as possible to one of the field traces. In case two or more components are analysed jointly, the inversion scheme we adopt is based on the Pareto optimality and aims at finding models that represent the best compromise with respect to the two (or more) considered objective functions (Dal Moro, Moura, and Moustafa 2015a; Pardalos, Migdalas, and Pitsoulis 2008; Ramík and Vlach 2002; Dal Moro, Ponta, and Mauro 2015b; Dal Moro et al. 2016, 2018). Figure 4 reports an example of bi-objective space where each model evaluated during the optimisation procedure is identified by its misfits (in our case, the first misfit refers to the radial component of Rayleigh waves

Table 1. Nomenclature adopted for the different components (i.e. acquisition settings). See also Figure 2 and Dal Moro (2014).

Acronym	Geophone	Source	Component
ZVF	Vertical (Z)	Vertical force (sledgehammer, weight drop, vibroseis)	Vertical component of Rayleigh waves
ZEX	Vertical (Z)	Explosive	Vertical component of Rayleigh waves
RVF	Horizontal with axis parallel to the array - radial (R) component (Figure 2a)	Vertical Force (sledgehammer, weight drop, vibroseis)	Radial component of Rayleigh waves
REX	Horizontal with axis parallel to the array - radial (R) component	Explosive	Radial component of Rayleigh waves
THF	Horizontal with axis perpendicular (transversal, T) to the array (Figure 2a)	Shear source (horizontal force)	Love waves

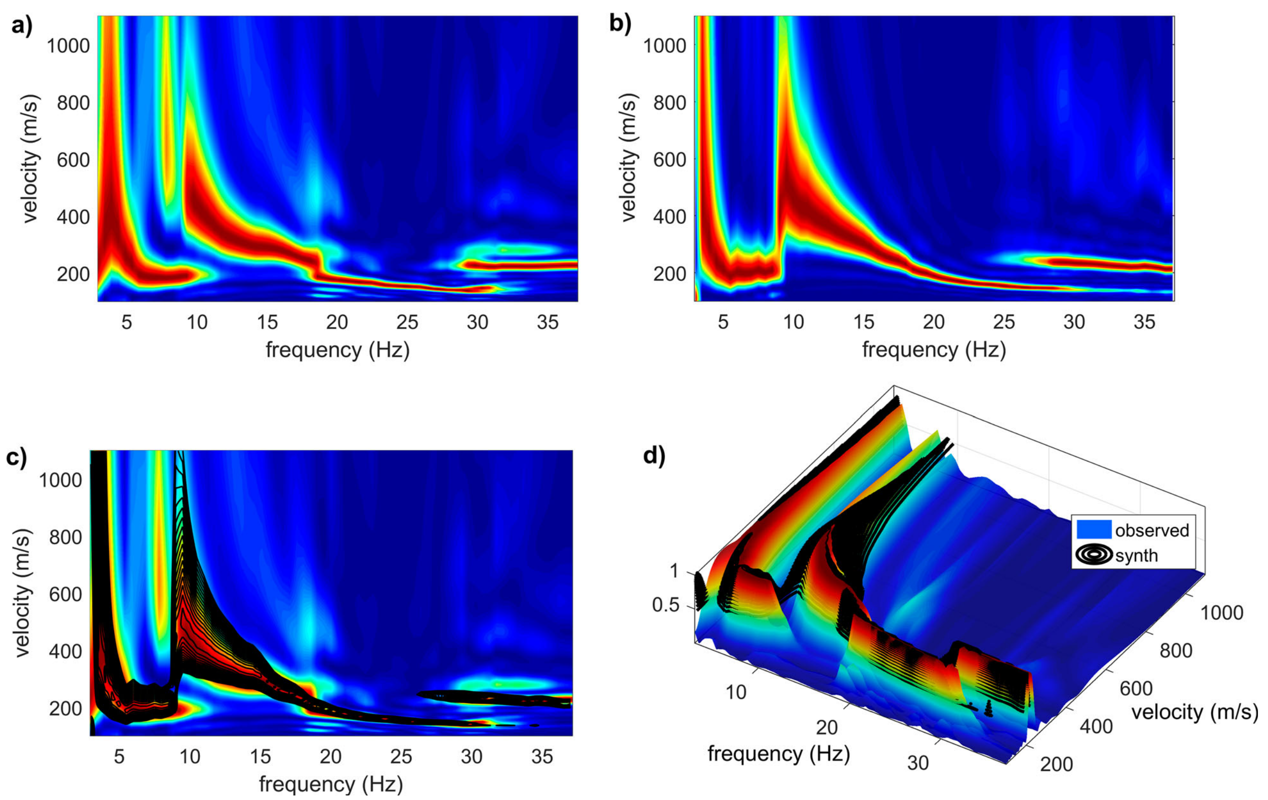

Figure 3. Example of single-component FVS analysis: (a) phase–velocity spectrum of a field data set; (b) phase–velocity spectrum of the model identified through the inversion procedure described in this paper; (c) compact representation of the two previous velocity spectra (background colours represent the velocity spectrum of the field data, whereas the overlaying black contour lines relate to the synthetic one); (d) same data as in the previous plot but from a different (3D) perspective.

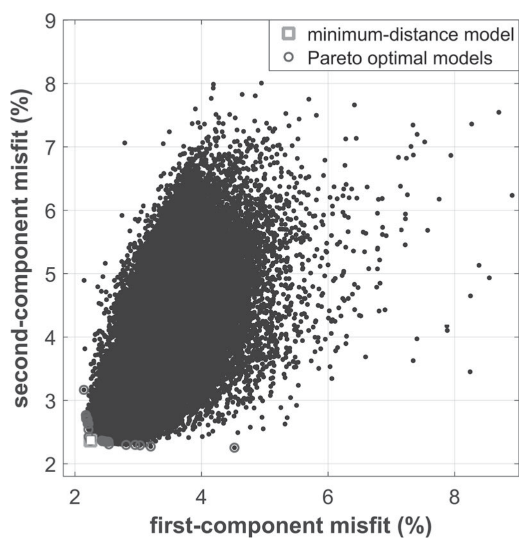

Figure 4. MOEA optimisation: bi-objective space. Each point represents a model evaluated during the optimisation procedure. Circles indicate the final Pareto-optimal models and the square highlights the minimum-distance model (i.e. the model with the minimum geometrical distance from the ideal utopia point). Further details in Dal Moro and Pipan (2007).

and the second to Love waves). A description of this type of multi-objective evolutionary algorithms (MOEA) optimisation scheme is provided in Van Veldhuizen and Lamont (2000), Coello (2003), Dal Moro and Pipan (2007) and Dal Moro and Ferigo (2011).

The proposed approach through a case study

The data set was acquired in northwest Italy (Figure 5) in the framework of the geotechnical characterisation of a construction area. The site is located along a Quaternary river terrace composed mainly of soft sediments (silt, clay and sand), alternating with deposits of polygenic gravels that may be occasionally cemented (conglomerates). Active data were acquired by means of 22 4.5 Hz horizontal geophones and an 8-kg sledgehammer (Table 2 and Figure 6). As described widely in Dal Moro (2014) and recalled briefly in the introductory paragraph, horizontal geophones allow the efficient acquisition of both the radial component of Rayleigh waves (RVF) and Love waves (THF component). Figure 6 reports the original data (seismic traces and phase–velocity spectra computed via phase shift; Park, Miller, and Xia 1998), whereas in Figure 7 we show the velocity spectra of the decimated data sets obtained by removing each second trace (thus keeping only 11 traces). By comparing the phase–velocity spectra in Figures 6 and 7, three facts can be highlighted:

(1) for the RVF component, the higher modes apparent at frequencies higher than ∼ 35 Hz are slightly more evident in the velocity spectrum computed from the decimated data set (white box in Figure 7b);

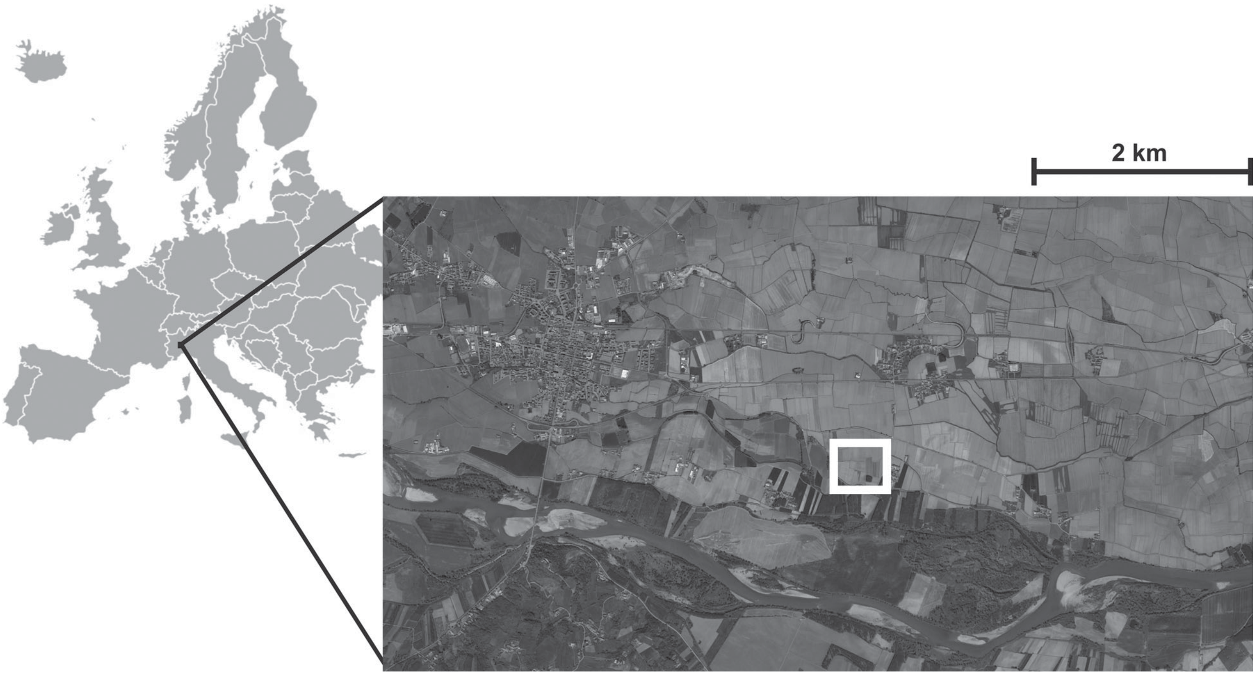

Figure 5. Location of the site (northwest Italy). In the lower part of the map is visible the River Po.

Table 2. Acquisition parameters.

Number of channels	22
Sampling rate	1 ms
Record time	1 s
Geophone spacing	2 m
Minimum offset	7 m
Stack	5

(2) spatial aliasing shows up in the THF velocity spectrum (for frequencies higher than ~ 45 Hz and velocities larger than ~ 400 m/s) (Figure 7d);
(3) the dispersive properties are clearly and properly imaged even by considering only 11 traces.

Since the FVS approach is computationally demanding, dealing with a lighter data set (composed by only 11 traces) is surely useful (computational times are reduced) and the only caution we might consider is reducing the frequency range up to ~ 45 Hz to avoid spatial aliasing (which would not represent a problem cause the synthetics would also reproduce it). In this regard, it must be considered that from the geological/engineering point of view, 45 Hz are already an extremely high frequency that relates to the layers down to about two decimetres and are then quite irrelevant.

As underlined in Dal Moro et al. (2003) and Dal Moro (2014), when the dispersive properties are imaged via phase shift and not through the f–k transform (which compared with the phase shift method is much more influenced by spatial aliasing), the actual number of traces is not relevant. These means that, for common geotechnical applications (array length between about 40 and 70 m) a limited number of channels (in this case we used 11 traces) is sufficient and the deployment of more geophones would result in longer field procedures without any increase in the information actually exploited during the data analysis. The velocity spectra in Figure 7(b) and 7(d) are equivalent to the velocity spectra in Figure 6(b) and 6(d) but because we are processing the spectra according to the FVS approach, using fewer traces will also reduce the computational load.

Figure 8 presents the results of the accomplished joint FVS inversion. The field and synthetic velocity spectra for both the considered components are shown and the overall consistency between field and synthetic data is apparent. In order to give evidence of the complexity of Rayleigh waves and the consequent importance of the adopted joint FVS analysis, in Figure 9 we report the modal dispersion curves of the identified model (shown in Figure 8c). Two facts are particularly important. Between 7 and 15 Hz, the Rayleigh-wave spectrum (Figure 9a) is not representative of any specific mode but is rather a mix between the fundamental and the first higher mode. Furthermore, for frequencies lower than about 6 Hz the energy relates to the second and third higher modes which dominate the spectra also for frequencies higher than 20 Hz.

By contrast, the THF phase–velocity spectrum is very well focused and, for frequencies higher than 5 Hz, clearly representative of the fundamental mode alone.

It is often suggested that the maximum penetration depth of a MASW survey is defined by half of the largest identified wavelength (Shtivelman 2003). As a matter of fact, the actual penetration cannot be defined in a precise way because the sensitivity is decreasing slowly with depth and the idea of an exact depth is therefore necessarily naive. However, because the specific features of the velocity spectrum depend also on the

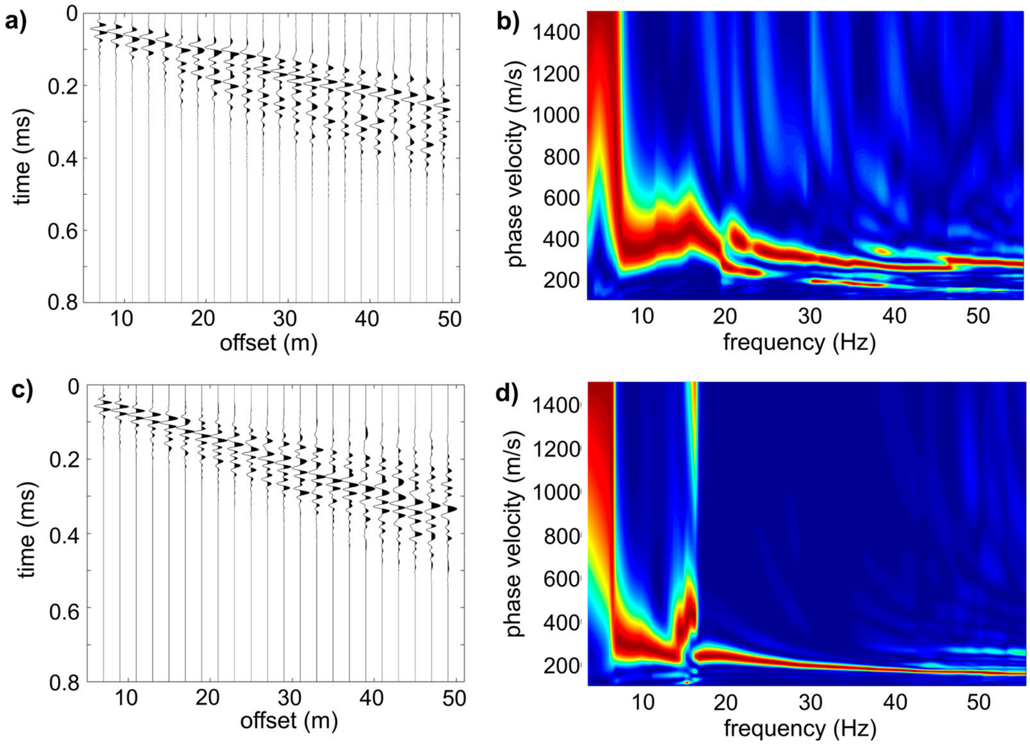

Figure 6. Original (22 traces) field data set: (a) Rayleigh waves (radial component – RVF) and (b) its phase–velocity spectrum; (c) THF component (Love waves) and (d) its phase–velocity spectrum.

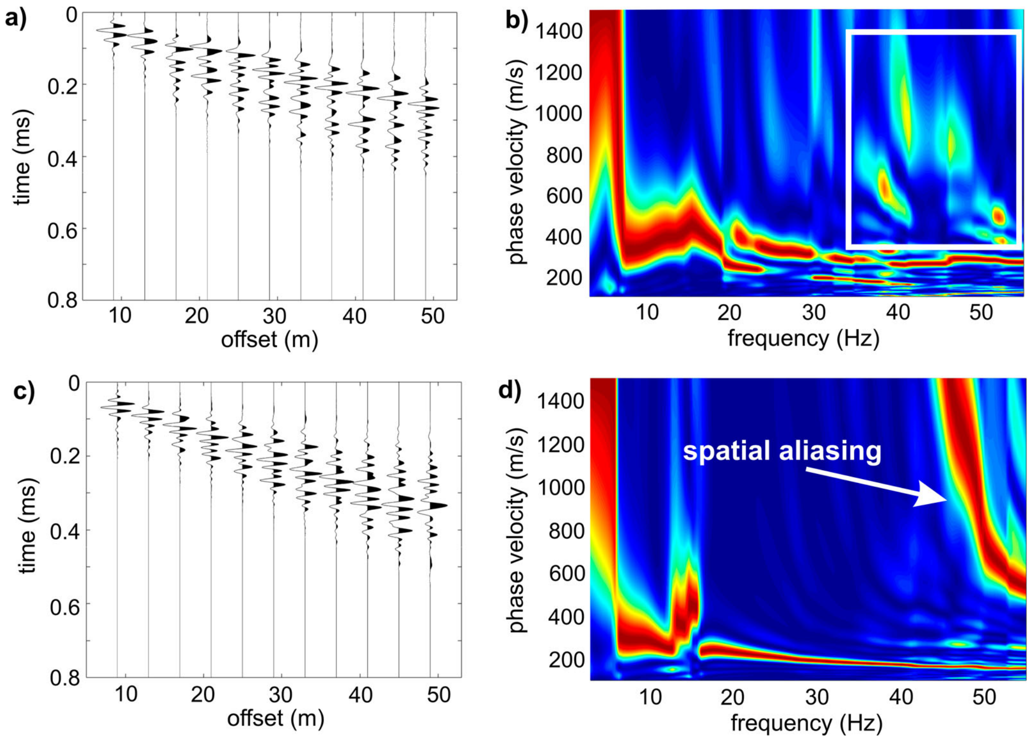

Figure 7. Decimation of the traces reported in Figure 6(a) and 6(c). For both the RVF (a) and THF (c) components only 11 traces are now kept. In spite of this, the phase–velocity spectra obtained from the decimated data sets are fundamentally identical to those obtained while considering 22 traces. For further details see text.

length of the array, a common rule of thumb assumes that the penetration depth is approximately half of the array length.

It is clear that below 5 Hz, the velocity increases suddenly (see Figure 6b and 6d) thus providing the evidence that at a certain depth (that the inversion process identified in about 18 m), an abrupt V_S increase occurs and reaches values typical of the conglomerates. By contrast, the V_S profile below such a stratigraphic contact can be considered as merely speculative because the length of the array (42 m) does not allow a greater penetration depth.

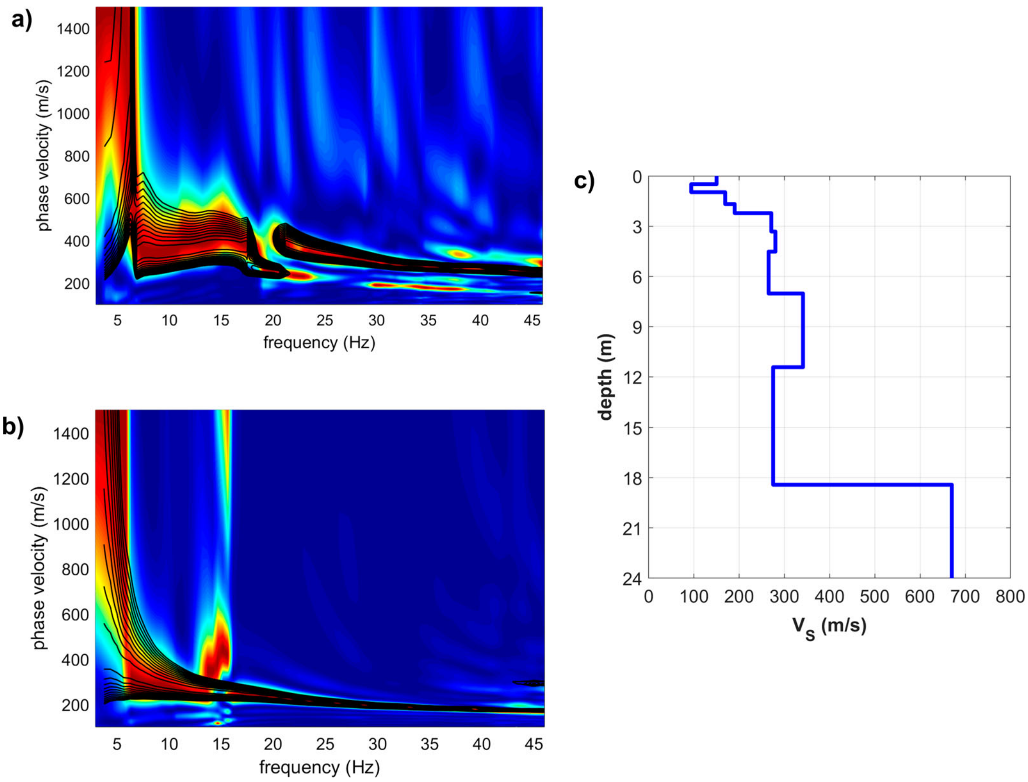

Figure 8. Result of the joint FVS analysis of the RVF and THF components: (a) radial component of Rayleigh waves (the colours in the background relate to the field data while the overlaying black contour lines represent the velocity spectrum of the identified model); (b) Love waves; (c) identified V_S vertical profile.

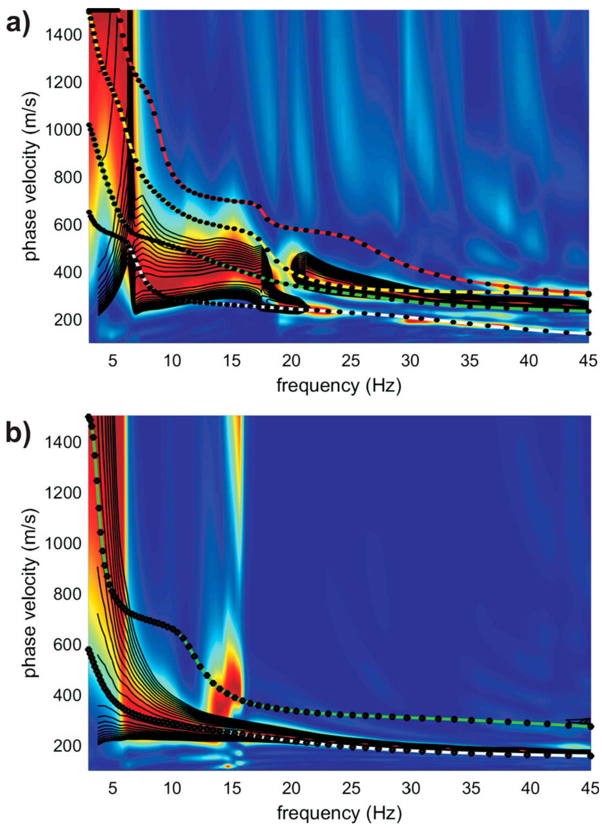

Figure 9. Observed (background colours) and synthetic (overlaying black contour lines) phase–velocity spectra for the two considered components and theoretical modal dispersion curves of the subsurface V_S model reported in Figure 8(c): (a) the first four modes for the radial component of Rayleigh waves; (b) the first two modes for Love waves. See text for comments.

It must be also considered that the signal below 5 Hz does not pertain to the fundamental mode but to the second overtone (Figure 9a). All these facts suggest that, reasonably and roughly speaking, the maximum depth that can be investigated by the considered data is not larger than about 23 m.

In other words, we can be sure that a massive conglomerate is present at a depth of $\sim$ 18 m, but we cannot say much about its thickness.

For the shallowest part, we compared the obtained shear-wave velocities with penetrometer data obtained $\sim$ 40 m away from the centre of the seismic array by means of a dynamic probing super heavy (DPSH) test (Stefanoff et al. 1989) performed to characterise the site from the geotechnical point of view (Figure 10). At a depth of $\sim$ 2 m, the increase in V_S and N_{20} (number of blows required to penetrate 20 cm) shows the contact between the superficial soft soil (silt/clay) and a series of stiffer sandy layers, while considering the stratigraphic characteristic of the area, the value of V_S at a depth of 18 m indicates the presence of conglomerates.

In general terms, it must be considered that penetrometer tests and borehole seismics provide very local information, whereas MASW data depict the average model along the array (in this case 42 m long). For this reason, it is not always possible to establish a simple and perfect correlation between the obtained V_S values and the local penetrometer data (or the velocities determined via vertical seismic profiling). This is particularly relevant in areas where significant lateral variations

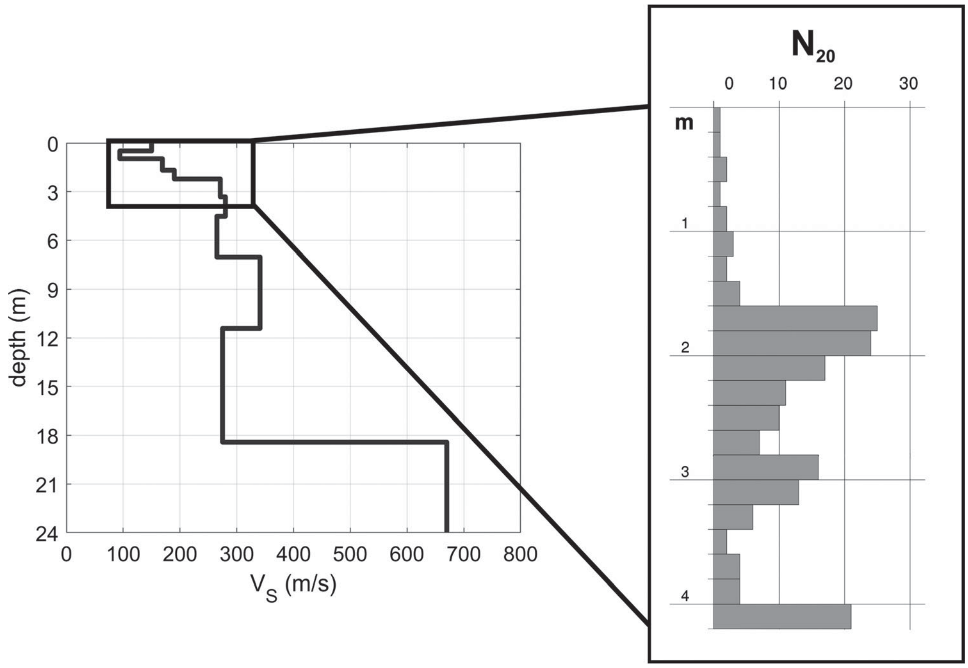

Figure 10. Geotechnical characterisation of the shallowest layers by means of a DPSH penetrometer test (N_{20} is the number of blows required to penetrate 20 cm) and the V_S profile obtained by means of the joint FVS analysis.

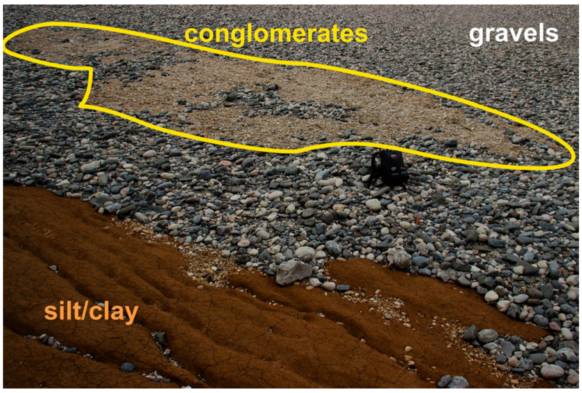

Figure 11. Riverbed about 1 km from the study area (consider that the Po river is responsible for the sedimentary characteristics of a very large area that also includes the one considered for the present study). Owing to the river dynamics, these high-plain areas can be quite complex from the sedimentary point of view. In this case, at the same level are present three distinct types of sedimentary materials: gravels, silt/clay sediments and conglomerates (area within the light line).

can occur (high-plain sedimentary river deposits; see Figure 11).

To further highlight the possible benefits of the approach proposed here (joint acquisition and FVS analysis of Rayleigh and Love waves), we processed the Rayleigh wave data while interpreting the main signal of the velocity spectrum (Figure 6b) as if belonging to a single mode (the fundamental one). This is the interpretation that would be inevitably given by anyone working with this component only (standard MASW approach). After picking the dispersion curve (see Figure 12a), we inverted it and obtained the V_S profile shown in Figure 12(b). This is the classical and common approach that would provide a seemingly good result: the picked dispersion curve and the one obtained from the inversion are in apparent good agreement.

Nevertheless, once we compute the Love wave dispersion curve of the model identified through this classical approach and compare it with the field velocity spectrum (Figure 12c), we realise that for frequencies lower than 15 Hz, the identified model is not consistent with the Love wave dispersion. Such a disagreement provides the evidence that the Rayleigh-wave picking (interpretation) was erroneous, although the inversion process of the picked dispersion curve provided a seemingly-good result (if we consider only the Rayleigh-wave data).

The inconsistency of this result should be compared with the outcome of the joint FVS inversion presented in Figure 8, where the velocity spectra of the identified model and the observed ones match quite well for both Rayleigh and Love waves.

In short, the approach presented here aims to avoid the pitfalls created by two mutually related problems: the use of a single component and its simplistic analysis in terms of modal dispersion curves.

Conclusions

Surface wave acquisition and analysis can be performed according to very different methodologies and the accuracy of the retrieved vertical V_S profile clearly depends on the overall adopted approach.

In past years, optimised acquisition procedures and comprehensive processing techniques have progressively increased the cost-effectiveness and accuracy of

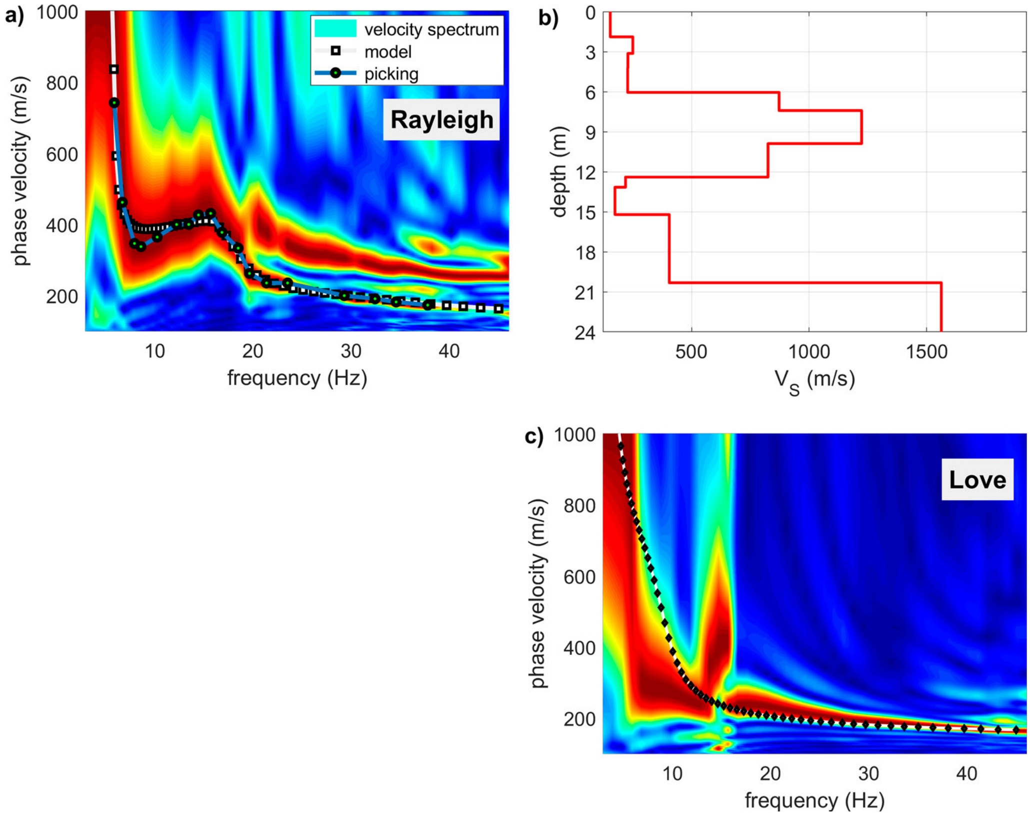

Figure 12. Usefulness of a second component (in this case Love waves) to check the consistency of the Rayleigh wave data interpretation in terms of modal dispersion curve: (a) Rayleigh wave velocity spectrum with the picked dispersion curve (interpreted as the fundamental mode) and the dispersion curve of the model obtained by inverting the picked curve; (b) V_S model obtained from the inversion of the picked dispersion curve; (c) Love waves: velocity spectrum with the dispersion curve of the model identified through the inversion of the Rayleigh wave dispersion curve. See text for comments.

the reconstructed subsurface model. From this perspective, we presented an approach based on the FVS joint analysis of the Rayleigh and Love waves acquired by means of a set of (4.5 Hz) horizontal geophones only. As shown, if the dispersive properties are obtained via phase shift, the number of necessary traces is smaller than is generally believed so that, for a common 40–100 m array, using 12 or 24 traces does not make any significant difference (see also the examples reported in paragraph 2.2.1 of Dal Moro 2014). What really matters is the total length of the array (i.e. the distance between the first and last geophones), which influences the depth to which the retrieved model is sufficiently focused and which is approximately equal to half the array length.

Although the FVS approach is computationally heavier if compared to the analysis of the modal dispersion curves, it can be adopted proficiently to analyse complex velocity spectra that cannot be otherwise soundly understood and interpreted in terms of modal dispersion curves.

Because phase shift allows to define the dispersive properties even while considering a limited number of traces, by using just 12 channels we obtain a twofold result:

(1) reduced field effort;
(2) reduced computation time for the FVS inversion process which, being based on the computation of the synthetic traces, is influenced by the number of considered channels.

For the present case study, the joint analysis of Rayleigh and Love waves was accomplished without the need to introduce any anisotropy ($V_{SH} = V_{SV}$). The overall good agreement of the obtained velocity spectra for both the RVF and THF components (see Figure 8) provides the evidence evidence that the local sediments are fundamentally isotropic (same properties along both the vertical and horizontal axes). This should not be surprising since the velocities identified down to 18 m are typical of silt/clay/sandy materials (likely mixed with a limited amount of gravels/pebbles) that do not have any apparent reason to behave anisotropically.

By contrast, if working in areas where, due to fractures, stratification or grain orientation, the isotropic case does not apply, the joint inversion process should allow a certain amount of anisotropy ($V_{SH} \neq V_{SV}$), always considering that it would be meaningless to invoke anisotropies whose values are smaller than the intrinsic uncertainty of the retrieved V_S values.

It is important to point out that for the present data (as for many others), the Rayleigh wave velocity spectrum would have been impossible to interpret in terms of modal dispersion curves because over a certain frequency range, the energy is actually a sort of mix between the fundamental and first higher modes (see Figure 8 and related comments and references).

Finally, in adopting the described approach (joint analysis of Love waves and the radial-component of Rayleigh waves) for the analysis of group velocities (e.g. Dal Moro et al. 2016; 2018; Dal Moro, Ponta, and Mauro 2015b; Dziewonsky, Bloch, and Landisman 1969; Ritzwoller and Lavshin 2003), we would just need one single horizontal geophone that, properly rotated, would allow the acquisition of Love waves as well as the radial component of Rayleigh waves.

Acknowledgements

This work was partly supported by the Institute of Rock Structure and Mechanics (Czech Academy of Sciences – Prague, CZ) in the framework of the long-term conceptual development project RVO 67985891 (Institute grant for the "Extreme Seismics" project). The author would like to express his gratitude to Luca Maria Puzzilli (ISPRA, Italy), Lorenz Keller (*roXplore*, Switzerland) and two anonymous reviewers whose comments significantly helped in improving the overall manuscript.

Disclosure statement

No potential conflict of interest was reported by the author.

Funding

This work was partly supported by the Institute of Rock Structure and Mechanics (Czech Academy of Sciences - Prague, CZ) in the framework of the long-term conceptual development project RVO 67985891 (Institute grant for the "Extreme Seismics" project).

ORCID

Giancarlo Dal Moro http://orcid.org/0000-0003-2009-6436

References

Aki, K. 1957. Space and time spectra of stationary stochastic waves, with special reference to microtremors. *Bulletin of Earthquake Research Institute* 35: 415–56.

Asten, M. 2006. On bias and noise in passive seismic data from finite circular array data processed using SPAC methods. *Geophysics* 71: V153–62. doi:10.1190/1.2345054.

Asten, M. W., A. Aysegul, E. E. Ezgi, S. F. Nurten, and U. Beliz. 2014. Site characterisation in north-western Turkey based on SPAC and HVSR analysis of microtremor noise. *Exploration Geophysics* 45: 74–85. doi:10.1071/EG12026.

Capon, J. 1969. High-Resolution frequency-Wavenumber spectrum analysis. *Proceedings of the IEEE* 57 no. 8: 1408–19.

Carcione, J. M. 1992. Modeling anelastic singular surfaces waves in the earth. *Geophysics* 57, no. S7: 781–92.

Cho, I., S. Senna, and H. Fujiwara. 2013. Miniature array analysis of microtremors. *Geophysics* 78, no. 1: KS13–23. doi:10.1190/geo2012-0248.1.

Coello Coello, C. A. 2003. Guest editorial: special issue on evolutionary multiobjective optimization. *IEEE Transactions on Evolutionary Computation* 7: 97–9.

Dal Moro, G. 2011. Some aspects about surface wave and HVSR analyses: a short overview and a case study. *Bollettino di Geofisica Teorica ed Applicata (BGTA)* 52: 241–59.

Dal Moro, G. 2014. *Surface wave analysis for Near surface applications*. Oxford, UK: Elsevier, ISBN 9780128007709.

Dal Moro, G., V. Coviello, and G. Del Carlo. 2014. Shear-Wave velocity reconstruction via unconventional joint analysis of seismic data: two case studies in the light of some theoretical aspects. *In* Engineering Geology for Society and Territory - Volume 5 - Springer International Publishing. pp. 1177–82.

Dal Moro, G., and F. Ferigo. 2011. Joint analysis of Rayleigh and Love wave dispersion for Near-surface studies: issues, Criteria and Improvements. *Journal of Applied Geophysics* 75: 573–89.

Dal Moro, G., L. Keller, S. R. Moustafa, and N. Al-Arifi. 2016. Shear-wave velocity profiling according to three alternative approaches: a comparative case study. *Journal of Applied Geophysics* 134: 112–24.

Dal Moro, G., R. M. Moura, and S. R. Moustafa. 2015a. Multi-component joint analysis of surface waves. *Journal of Applied Geophysics* 119: 128–38.

Dal Moro, G., S. R. Moustafa, and N. Al-Arifi. 2018. Improved Holistic analysis of Rayleigh waves for single- and multi-offset data: joint inversion of Rayleigh-wave Particle Motion and vertical- and radial-component velocity spectra. *Pure and Applied Geophysics* 175: 67–88.

Dal Moro, G., and M. Pipan. 2007. Joint inversion of surface wave dispersion curves and reflection Travel times via multi-objective evolutionary Algorithms. *Journal of Applied Geophysics* 61: 56–81.

Dal Moro, G., M. Pipan, E. Forte, and I. Finetti. 2003. Determination of Rayleigh wave dispersion curves for near surface applications in unconsolidated sediments: In Proceedings SEG, 73st Annual Int. Mtg. (Dallas, Texas).

Dal Moro, G., R. Ponta, and R. Mauro. 2015b. Unconventional optimized surface wave acquisition and analysis: Comparative tests in a Perilagoon area. *Journal of Applied Geophysics* 114: 158–67.

Dou, S., and J. B. Ajo-Franklin. 2014. Full-wavefield inversion of surface waves for mapping embedded low-velocity zones in permafrost. *Geophysics* 79, no. 6: EN107–24.

Dziewonsky, A., S. Bloch, and N. Landisman. 1969. A technique for the analysis of transient seismic signals. *Bulletin of the Seismological Society of America* 59: 427–44.

Forbriger, T. 2003a. Inversion of shallow-seismic wavefields: I. wavefield transformation. *Geophysical Journal International* 153: 735–52.

Forbriger, T. 2003b. Inversion of shallow-seismic wavefields: II. Inferring subsurface properties from wavefield transforms. *Geophysical Journal International* 153: 735–52.

Ganji, V., N. Gucunski, and S. Nazarian. 1998. Automated inversion procedure for spectral analysis of surface waves. *Journal of Geotechnical and Geoenvironmental Engineering* 124, no. 8: 757–70.

Gao, L., J. Xia, Y. Pan, and Y. Xu. 2016. Reason and condition for mode kissing in MASW method. *Pure and Applied Geophysics* 173, no. 5: 1627–38.

Herrmann, R. B. 2015. Computer Programs in Seismology. Open files: http://www.eas.slu.edu/People/RBHerrmann/CPS330.html [last accessed May 2018].

Ivanov, J., R. D. Miller, J. Xia, D. Steeples, and C. B. Park. 2006. Joint analysis of refractions with surface waves: an inverse refraction-traveltime solution. *Geophysics* 71: R131–8.

Ling, S., and H. Okada. 1993. *An extended use of the spatial autocorrelation method for the estimation of geological structure* *using microtremors*. Proceedings of the 89th SEGJ Conference, 44–48 (in Japanese).

Louie, J. N. 2001. Faster, better: shear wave velocity to 100 meters depth from refraction microtremors arrays. *Bulletin of the Seismological Society of America* 91: 347–64.

Miller, G. F., and H. Pursey. 1955. On the partitioning of energy between elastic waves in a semi-infinite solid. *Proceedings of the Royal Society of London, Series A* 233: 55–69.

Ohori, M., A. Nobata, and K. Wakamatsu. 2002. A comparison of ESAC and FK methods of estimating phase velocity using arbitrarily shaped microtremor analysis. *Bulletin of the Seismological Society of America* 92: 2323–32.

Pardalos, P.M., Migdalas, A., and Pitsoulis, L., eds. 2008. *Pareto optimality, Game Theory and Equilibria*. New York: Springer-Verlag, ISBN 978-0-387-77247-9

Park, C. B., R. D. Miller, and J. Xia. 1998. Imaging dispersion curves of surface waves on multichannel record. 68th Annual International Meeting Society of Exploration Geophysicists, Expanded Abstracts, 1377–80.

Park, C. B., R. D. Miller, and J. Xia. 1999. Multichannel analysis of surface waves. *Geophysics* 64: 800–08.

Park, C. B., R. D. Miller, J. Xia, and J. Ivanov. 2000. Multichannel seismic surface-wave methods for geotechnical applications. In Proceedings of the First International Conference on the Application of Geophysical Methodologies to Transportation Facilities and Infrastructure, St. Louis, December 11–15.

Poggi, V., and D. Fäh. 2010. Estimating Rayleigh wave particle motion from three-component array analysis of ambient vibrations. *Geophysical Journal International* 180: 251–67. doi:10.1111/j.1365-246X.2009.04402.x.

Ramík and Vlach. 2002. Pareto-optimality of compromise decisions. *Fuzzy Sets and Systems* 129: 119–27.

Ritzwoller, M. H., and A. L. Lavshin. 2003. Estimating shallow shear velocities with marine multicomponent seismic data. *Geophysics* 67: 1991–2004.

Ryden, N., and C. B. Park. 2006. Fast simulated annealing inversion of surface waves on pavement using phase-velocity spectra. *Geophysics* 71: R49–58.

Safani, J., A. O'Neill, T. Matsuoka, and Y. Sanada. 2005. Applications of Love wave dispersion for Improved shear-wave velocity Imaging. *Journal of Environmental and Engineering Geophysics* 10: 135–50.

Shtivelman, V. 2002. Surface wave sections as a tool for imaging subsurface inhomogeneities. *European Journal of Environmental and Engineering Geophysics* 7: 121–38.

Shtivelman, V. 2003. Using surface waves for studying the shallow subsurface. *Bollettino di Geofisica Teorica ed Applicata* 44: 223–36.

Stefanoff, G., Sanglerat, G., Bergdahl, U., and Melzer, K. (Technical Comm. on Penetration Testing of the International Society for Soil Mechanics and Foundations Engineering, ISSMFE). 1989. Dynamic Probing (DP): International Reference Test Procedure, Penetration Testing 1988, ISOPT-1, De Ruiter (ed.) 1988, Balkema, Rotterdam, ISBN 9061918014.

Stokoe, K. H. I. I., S. Nazarian, G. J. Rix, I. Sanchez-Salinero, J. Sheu, and Y. Mok. 1988. In situ seismic testing of hard-to-sample soils by surface wave method. Earthq. Eng. and soil Dyn. II - Recent adv. in ground-motion eval. - Park City. *American Society of Civil Engineers*, 264–77.

Van Veldhuizen, D. A., and G. B. Lamont. 2000. Multiobjective evolutionary algorithms: analyzing the state-of-the-art. *Evolutionary Computation* 8: 125–47.

Winsborrow, G., D. G. Huwsa, and E. Muyzert. 2003. Acquisition and inversion of Love wave data to measure the lateral variability of geo-acoustic properties of marine sediments. *Journal of Applied Geophysics* 54: 71–84.

Xia, J., Y. Xu, C. Chen, R. D. Kaufmann, and Y. Luo. 2006. Simple equations guide high-frequency surface-wave investigation techniques. *Soil Dynamics and Earthquake Engineering* 26: 395–403.

Xia, J., Y. Xu, Y. Luo, R. D. Miller, R. Cakir, and C. Zeng. 2012. Advantages of using Multichannel analysis of Love waves (MALW) to Estimate Near-surface shear-wave velocity. *Survey in Geophysics* 33: 841–60. doi:10.1007/s10712-012-9174-2.

Zhang, S. X., and L. S. Chan. 2003. Possible effects of misidentified mode number on Rayleigh wave inversion. *Journal of Applied Geophysics* 53: 17–29.